Received February 1, 2021, accepted February 16, 2021, date of publication February 22, 2021, date of current version March 3, 2021.

Digital Object Identifier 10.1109/ACCESS.2021.3060746

Development and Metrological Evaluation of a Force Transducer for Industrial Application

AJAY PRATAP SINGH[1,2], SANJOY K. GHOSHAL[1], HARISH KUMAR[3], JONGHUN YOON[4], AND POONAM YADAV[4]

[1]Mechanical Engineering Department, Indian Institute of Technology - ISM, Dhanbad 826004, India
[2]Mechanical Engineering Department, Ajay Kumar Garg Engineering College, Ghaziabad 201009, India
[3]Department of Mechanical Engineering, National Institute of Technology Delhi, Delhi 110040, India
[4]Department of Mechanical Engineering, BK21FOUR ERICA-ACE Center, Hanyang University, Ansan-si 15588, South Korea

Corresponding author: Jonghun Yoon (yooncsmd@gmail.com)

ABSTRACT The present investigation reports the development of a force transducer for industrial applications with facile design and manufacturing objectives. The design of the force transducer is based on the analytical and computational approaches, followed by the experimental verification. Factors such as stress, strain and deflection of the force transducer were evaluated while conducting a rigorous assessment of the proposed force transducer. Al 7075 (T6) grade of aluminum alloy has been used as the material for fabrication of the force transducer with a nominal capacity of 2 kN. The fabricated force transducer as per the proposed design has also been investigated for geometrical and dimensional accuracy using precision coordinate measuring machine (CMM). Metrological characterization as per ISO 376: 2011 revealed that uncertainty of measurements is within 0.05 %, which includes relative uncertainty of the force transducer the factors such as repeatability, reproducibility, reversibility, interpolation, resolution, zero offset. Based on the above investigations, it has been found that the designed force transducer is of low cost ($ 200–$ 300), ease to manufacturing, and precise enough (0.05 % uncertainty of measurement) force transducer for force measurement up to 2 kN. The developed force transducer offers sensitivity up to of 0.2 N or better.

INDEX TERMS Finite element analysis (FEA), ISO 376: 2011, metrological evaluation, square ring force transducer (SRFT), strain gauge.

I. INTRODUCTION

Conventionally, measurement systems have followed instrumentation for the measurement of force. A variety of sensors/transducers with a wide range of nominal capacities for the measurement of force, having numerous applications in many functional areas from N to MN force, are being used. In manufacturing applications, force transducers are needed for critical force measurements of functional grip by novel force transducers [1] e.g., bio-mechanic transducers. Moreover, force measurements using force transducers are widely utilized in various industrial applications such as aerospace, automobiles, and testing industries, amongst others. In manufacturing units, the optimization of a design in the machining process, by optimizing the mechanical force, shows significant improvement in resisting tool breakages and chatter control [2]–[4]. In addition, for precision positioning, a linear ultrasonic motor using a quadrate plate force transducer was developed. Furthermore, accuracy in prediction of chip loading on the machined surface relies on the measurement of mechanical forces. Therefore, the force transducer plays an important role in industry and academia [5]–[7]. The MEMS-based Infra-Red sensors have various benefits including low noise pollution, lightweight, smaller size, easy device/circuit interface, and they have vital and varied uses in civil and military fields [8]–[10]. Further, the current chip for low-pressure sensors was devolved using MEMS technologies and can only measure the pressure up to 500 Pa. These technologies have only been used for low pressure applications and are a very expensive technology [11], [12]. For drilling operations, the cutting force was measured for various types of material with different depth of cut and speed using a variety of tools [12], [13]. It is interesting that these force transducers are widely used in biomedical devices [14], [15] with different industrial applications, where low capacity force transducers are used [16], [17].

The associate editor coordinating the review of this manuscript and approving it for publication was Su Yan.

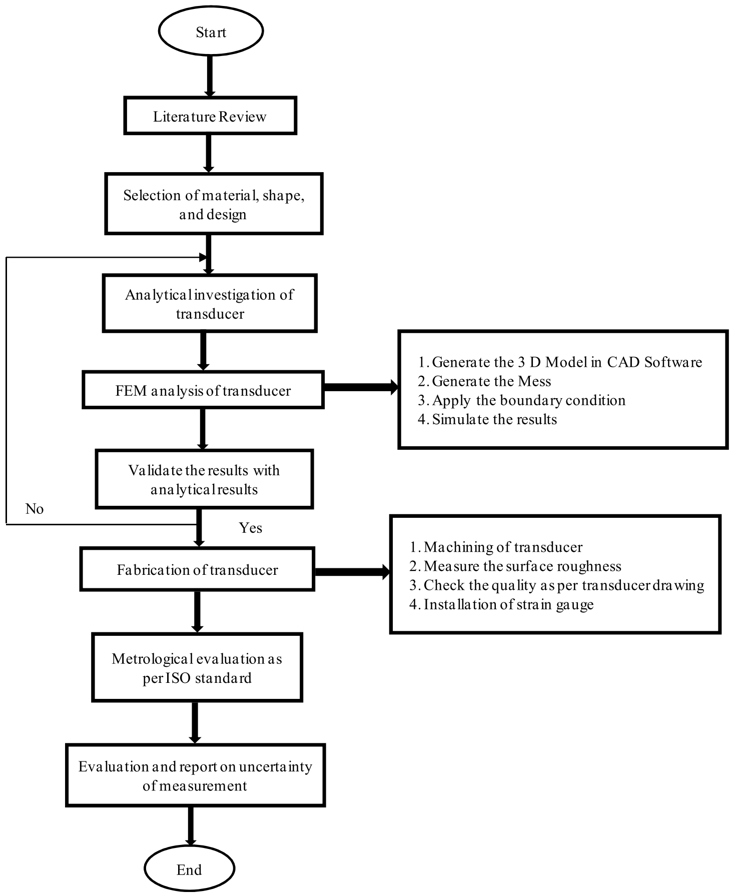

FIGURE 1. Schematic flow chart for design and development of the force transducer.

Further, miniature force/moments transducers (FMTs) are developed with 6 degrees of freedom (DOF) with a single sensor chip for use of instrumented teeth [18].

With growing technological requirements, developments are being made regarding the force transducer. There has been thrust push for development of precision force transducers, for different applications. To the best of the authors' knowledge, most precision force transducers are available commercially, and in developing nations such as India, they are generally imported for different applications. Such practice results in economic constraints and the cost of precision force transducers for uncertainty of measurement up to 0.05% may vary from \$500–1500 for a force transducer with nominal capacity of 1kN – 5 kN. Such force transducers are of complex shape, with limited scope of analytical or experimental validation of the design of the force transducer. Hence, the presented work aims to report the development of an in-house, low cost, simple, and precise force transducer for force measurement up to 2 kN. The developed force transducer offers sensitivity in the range of 0.2 N or better. The metrological characterization of the force transducer shows the suitability of the force transducer for a variety of applications, including mechanical, automation, laboratory, and medical [19]–[21]. It is evident from above mentioned literature regarding the development of a force transducer for industrial application that the square dimension is not still discussed for the development of an in-house, low cost, simple, and precise force transducer for force measurement up to 2 kN. Coordinate Measuring Machine (CMM) is also used for the dimensional measurement of the square shape force transducer ring. The major novelty of the current study also involves the square dimensioning along with the material AL 7075 (T6). The full version of ANSYS 16.0 has been used for the validation of the estimated results. The results might be useful to researchers and professionals to widen the applications of the force transducer.

II. DEVELOPMENT OF FORCE TRANSDUCER USING ANALYTICAL, COMPUTATIONAL AND EXPERIMENTAL APPROACHES

Figure 1 discusses the procedure adopted for design and development of the force transducer. The procedure includes analytical and computational approaches followed by validation through experimental measurements.

A. ANALYTICAL STUDY

Figure 2a shows the circular ring that is symmetrical around both axes of a ring force transducer. A quarter of the ring was used due to the symmetry of the ring, as shown in Figure. 2b.

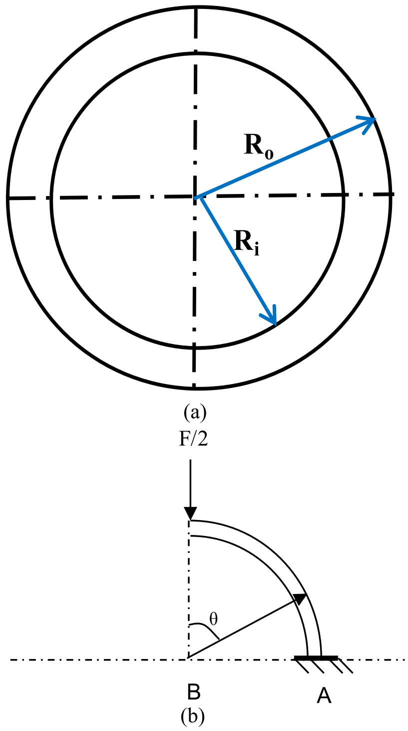

FIGURE 2. (a) Schematic of force transducer of ring shape. (b) A quarter of the ring.

As per the free body diagram the axial force (F) is applied to the ring, one end is free and other end (A) of the quarter circle is fixed without rotation. Thus, according to Castigliano's second theorem, we get [22]–[25],

$$\frac{\partial U}{\partial M_A} = 0 \tag{1}$$

Subsequently, a small increment of the ring section between the angles θ and dθ is considered. The bending moment (M) for this section is as follows.

$$M = M_A - \frac{F(R-x)}{2}$$

where, M_A = Moment at point A,, $x = R\cos\theta$

$$M = M_A - \frac{F(R - R\cos\theta)}{2} \tag{2}$$

Further, we know that the strain energy, (U), is

$$U = \int_0^{\pi/2} (\frac{M^2 ds}{2EI})$$

as, $ds = Rd\theta$

$$U = \int (\frac{M^2 R d\theta}{2EI}) \tag{3}$$

The partial derivative of U with respect to M_A must be zero for equation (1)

$$\frac{\partial U}{\partial M_A} = \frac{R}{EI}\int_0^{\pi/2} M\frac{\partial M}{\partial M_A} d\theta \tag{4}$$

Similarly, from eq. (2), we obtain

$$\frac{\partial U}{\partial M_A} = 1\int_0^{\pi/2} M^2 R d\theta = \int_0^{\pi/2} M - \frac{FR}{2}(1-\cos\theta) = 0$$

Integrating for given limits and solving for $M_A(\theta = \pi/2)$, we get

$$M_A = \frac{FR}{2}(1 - \frac{2}{\pi})$$
$$M_A = FR(\frac{1}{2} - \frac{2}{\pi}) \tag{5}$$

or,

$$M_A = 0.182FR \tag{6}$$

Substitute the value of M_A in eq. (2), and M becomes

$$M = \frac{FR}{2}(\cos\theta - \frac{2}{\pi}) \tag{7}$$

As per Castigliano's second theorem, the partial derivative of strain energy, U, with respect to a load, yields the displacement component of the loaded point in the direction of that load.

$$\delta_i = \frac{\partial U}{\partial F}, \ldots\ldots\ldots \quad (i = 1, 2, \ldots .n) \tag{8}$$

We find the deflection for the ring to be

$$\delta = \delta_i = \frac{FR^3}{EI}\left(\frac{\pi}{4} - \frac{2}{\pi}\right) \tag{9}$$

A force transducer of a square ring shape has been proposed and demonstrated as a modification of the force transducer of the ring shape. The ring's outer section is square while the inner portion is circular. The force transducer's outer surface offers ease of installing a strain gauge, while the inner ring offers suitability for a dial gauge. Researchers have discussed ring shape force transducers and derived appropriate systematic equations for calculating of strain (ε), stress (σ), and deflection (δ) for a square ring force transducer. In the current study, for the analysis of the stress, strain, and deflection, the similar equation also applies in the development & characterization of a square ring shaped force transducer along with the role of stress analysis by the previous researchers [2], [24]. Such a force transducer offers simple manufacturing and design considerations. The square ring design has been studied analytically as well as computationally (Figure 3). These equations provide an estimated value for δ, σ, and ε, when essential parameters are well - known, i.e., R, E, and F.

The equations for determining the estimated value of δ, σ, and ε of the force transducer [2], [24], are shown below.

$$\sigma = \frac{1.5M}{bt^2} \tag{10}$$
$$\varepsilon = \frac{1.5M}{Ebt^2} \tag{11}$$
$$\delta = \frac{0.9FR^3}{Ebt^3} \tag{12}$$

TABLE 1. Details of dimension and material specification.

Sl. No.	Quantity	Notation	Unit	Value
a	Radius(Internal circle)	R_i	mm	86
b	Radii (Outer)	R_o	mm	96
c	Radii (Mean)	R	mm	91
d	Thickness	t	mm	10
e	Width	b	mm	35
f	Modulus of elasticity	E	GPa	70.7
g	Poisson ratio	υ	--	0.33
h	force applied on transducer	F	N	2 000
i	Deflection for applied force (2 kN) using equation 12	δ	mm	0.541

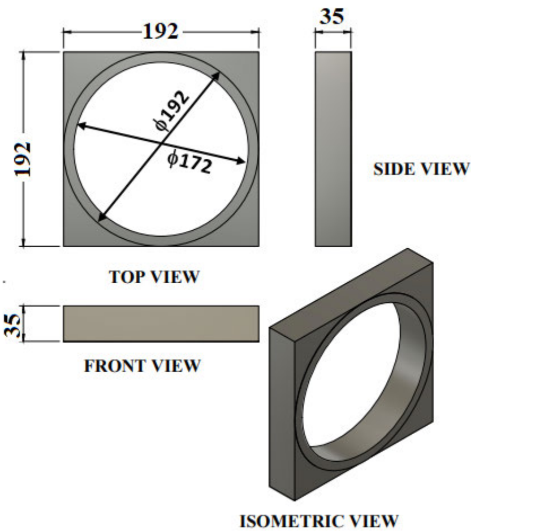

FIGURE 3. 3-Dimensional representation of square ring force transducer.

To develop the presented force transducer, AL7075 (T6) material was used. The internal diameter of the transducer ring has been finalized after optimization of design and fitting the dial gauge inside the internal circle to calculate the deflection. AL 7075 (T6) has good machinability, fatigue strength and is very strong compared to many steels. AL 7075 (T6) aluminum alloys are used in various industrial applications like aerospace, defense applications, automobiles, submarines, gears, and shafts, regulating valve parts, turbines, missile parts, keys, aircraft, and all-terrain vehicle (ATV) sprockets [26]–[28]. The details of dimensions and material properties are shown in Table 1.

B. COMPUTATIONAL FORCE TRANSDUCER ANALYSIS

The software ANSYS 16.0 was used to conduct computational investigations of the square ring force transducer (SRFT). A 3-D model has been designed for SRFT using

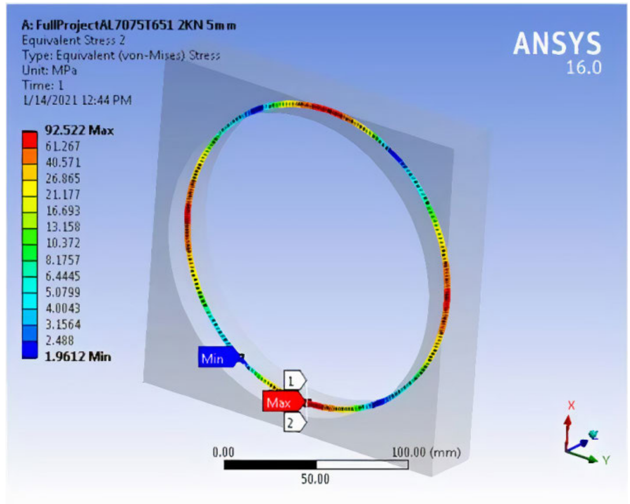

FIGURE 4. Stress over the square ring force transducer.

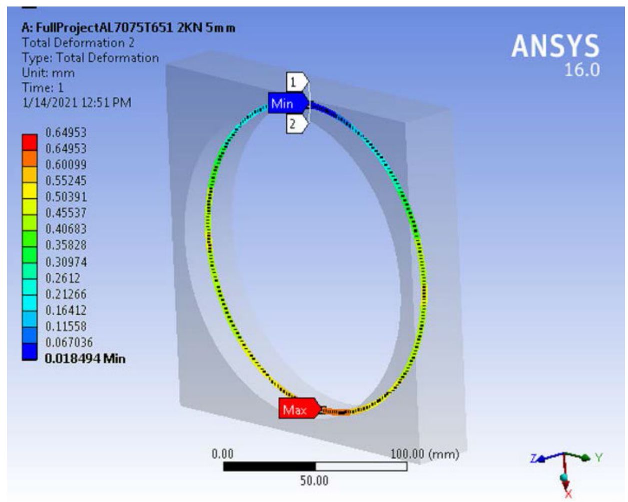

FIGURE 5. Deformation over the square ring force transducer.

the Solid edge software and simulation work has been completed on ANSYS software. For the computational study, the properties of Aluminum 7075 (AL7075 T6) including a Poisson ratio of 0.33 and Young's modulus of elasticity 71.7 GPa, have been used. The geometry and material have been assumed to be isotropic throughout the design. The desirable capacity of the SRFT is 2 kN and as per the analytical method, boundary conditions have been applied for the FEA. A total of 515815 elements and 727559 nodes were included and the size of the mesh was set to 5 mm during the SRFT investigations [29]. The meshing of SRFT is shown in Figure 12b. The element size was obtained from the standard library in the software, with curvature control having a maximum deviation factor of 0.1. The same methodology used for FEA of the SRFT, was implemented, and the deflection, stress, and strain patterns are drawn.

The FEA helps in obtaining stress-strain and deflection patterns for the SRFT and suitable locations for strain gauges' application. Figure 4 and 5 summarize deflection and stress

TABLE 2. Various parameters of machining.

S. No	Specification	Dimension value
1	Spindle speed	3000 revolution/min
2	Feed rate	1500 mm/min
3	Depth of cut	0.3–0.6 mm
4	Types of tools used	Carbide End mill diameter 12 mm; End mill cutter diameter 50 mm

FIGURE 6. Machining of the square ring force transducer.

patterns, respectively [30]. The stress is found to be within permissible limits, while deflection at a nominal force of 2 kN is found to be 0.649 mm.

C. EXPERIMENTAL MEASUREMENT

SRFT was developed while taking the analytical and computational investigations into consideration. The machining operation was performed on a computer numeric control (CNC) milling machine (vertical) equipped with controller 828D of SIEMENS. These machines are four-axis milling machines including a rotary axis. During the machining process, the following specifications were taken as shown in Table 2 given below. Figure 6 show the machining of the transducer.

After the machining, the surface roughness and geometrical dimensions were measured. Additionally, the surface roughness on the outer side as well as the inner side was measured. The measurements are shown in Table 3, including the value for installation of strain gauge on the outer surface. For application of strain gauges, it is preferred to have a surface roughness up to 5 μm [31]. A glimpse of the process of surface measurement is shown in Figure 7a and 7b.

TABLE 3. Roughness measurement data sheet.

S. No	Total Evaluation Length	Speed of stylus (m/s)	Name of Parameter	Inner Surface (Circular	Outer Surface (Flat Surface)
1	16	0.3	Arithmetical mean roughness (Ra)	0.472	0.704
2			Ten-point mean roughness (Rz)	2.781	5.214

TABLE 4. Dimensional measurement data sheet.

S. No.	Name of Parameters	Results (mm)
1	Inner diameter	172.08
2	Width	35.01
3	Roundness	0.02
4	Straightness	0.0001
5	Perpendicularity	0.02
6	Parallelism	0.004
7	Total length (both side)	192.12
8	Flatness	0.02

In this case, the coordinate measuring machine (CMM) is used to measure the various geometrical dimensions and tolerance parameters after the machining work on the outer surface as well as the circular surface of the square ring. Applicable parameters were measured, and they are summarized in Table 4. The process of measurement is shown in Figure 8a -8b.

The dial gauge–based force transducers (force proving instruments) have inherent limitations of reversibility and non-interpolative measurements. During the evaluation of the metrological investigation of the square ring force transducer, 0.2 μm and 0.1 μm resolution dial gauges were used.

In this study, foil-type strain gauges were used, and the resistance of all four strain gauges (R = 350 Ω) with a gauge factor K = 2 was used. A Wheatstone bridge was formed by arranging the strain gauges as shown in Figure 9a.

Equation 13 shows the bridge in proper balance conditions with equal strains.

$$\frac{R_1}{R_2} = \frac{R_4}{R_3} \tag{13}$$

Strain gauges were installed at identified positions and are shown in Figure 9b, in line with the implications of finite element analysis [31]–[32]. The calibration of the force transducer has been accomplished through the use of a high-resolution digital indicator having10^{-5} mV/V of resolution. Figures 9b–9e show the different aspects of the force transducers and 5 kN deadweight force machine.

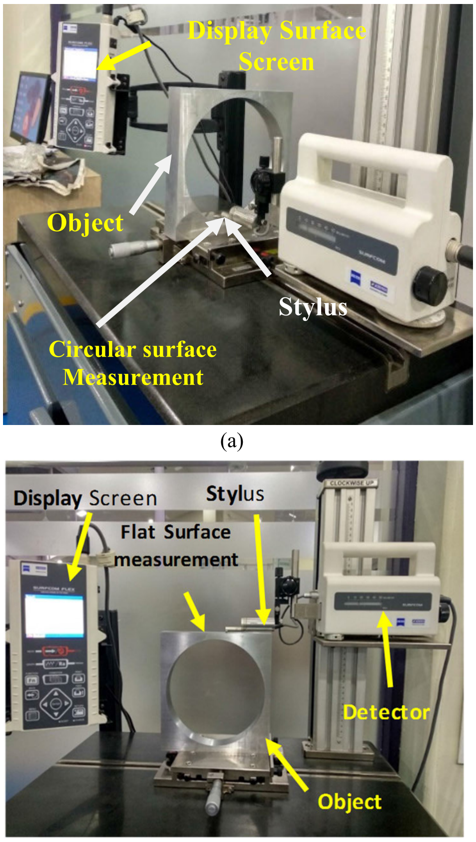

FIGURE 7. (a) Roughness measurement for circular inner surface. (b) Roughness measurement for outer flat surface.

D. COMPARISON OF DEFLECTION MEASUREMENT

For rigorous validation of the design methodology adopted, deflection has been evaluated for the different approaches viz., analytical, computational and experimental methods. The deflection is measured using a precision dial gauge of 0.1 μm resolution. The deflection is shown in Table 5, which summarizes that the deflection obtained from the experimental method is within 10 % of deviation to the analytical method and numerical method on either side of experimental measurements. The analytical expressions were formulated based on bending of curved bars; as such, they may not be practically valid for SRFT as the thickness is uniform in the case of the ring shaped force transducer. Figure 10 summarizes the salient findings of Table 5.

E. VALIDATION OF DESIGN THROUGH STRAIN MEASUREMENT COMPARISON

Four strain gauges (2 mm × 2 mm) were connected with two strain gauges connected along the Y axis in force direction, and the other two gauges were connected along the X axis, as shown in Figure 11. A full Wheatstone bridge configuration was formed using these four strain gauges. The different sensitivity of the force transducer is attributed to the arrangement of the strain gauge. A mathematical model is proposed to predict the sensitivity for different strain gauge arrangements.

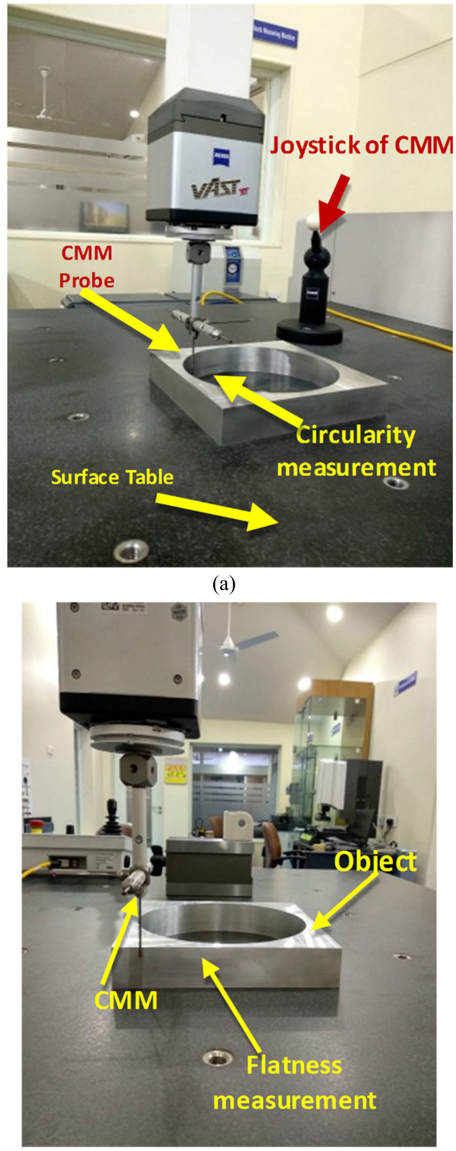

FIGURE 8. (a) Dimension measurement for inner circular surface. (b) Dimension measurement for outer flat surface.

The strain gauges forming the four arms of the full Wheatstone bridge consisting of resistances R_1, R_2, R_3 and R_4 with R_1 and R_3 measuring perpendicular strain and R_2 and R_4 measuring axial strains, then the output voltage (V_{out}) with respect to excitation voltage (V_{in}) is calculated by using Kirchhoff's law:

$$\frac{V_{out}}{V_{in}} = \frac{R_1}{R_1 + R_2} - \frac{R_4}{R_3 + R_4} \tag{14}$$

The resistance of all strain gauges (R = 350 Ω) and gauge factor (K = 2) have been taken giving an output of zero in a balanced condition for the bridge. However, with the variation in the application of force applied on the transducer, the resistance values were changed. The variation in resistance with

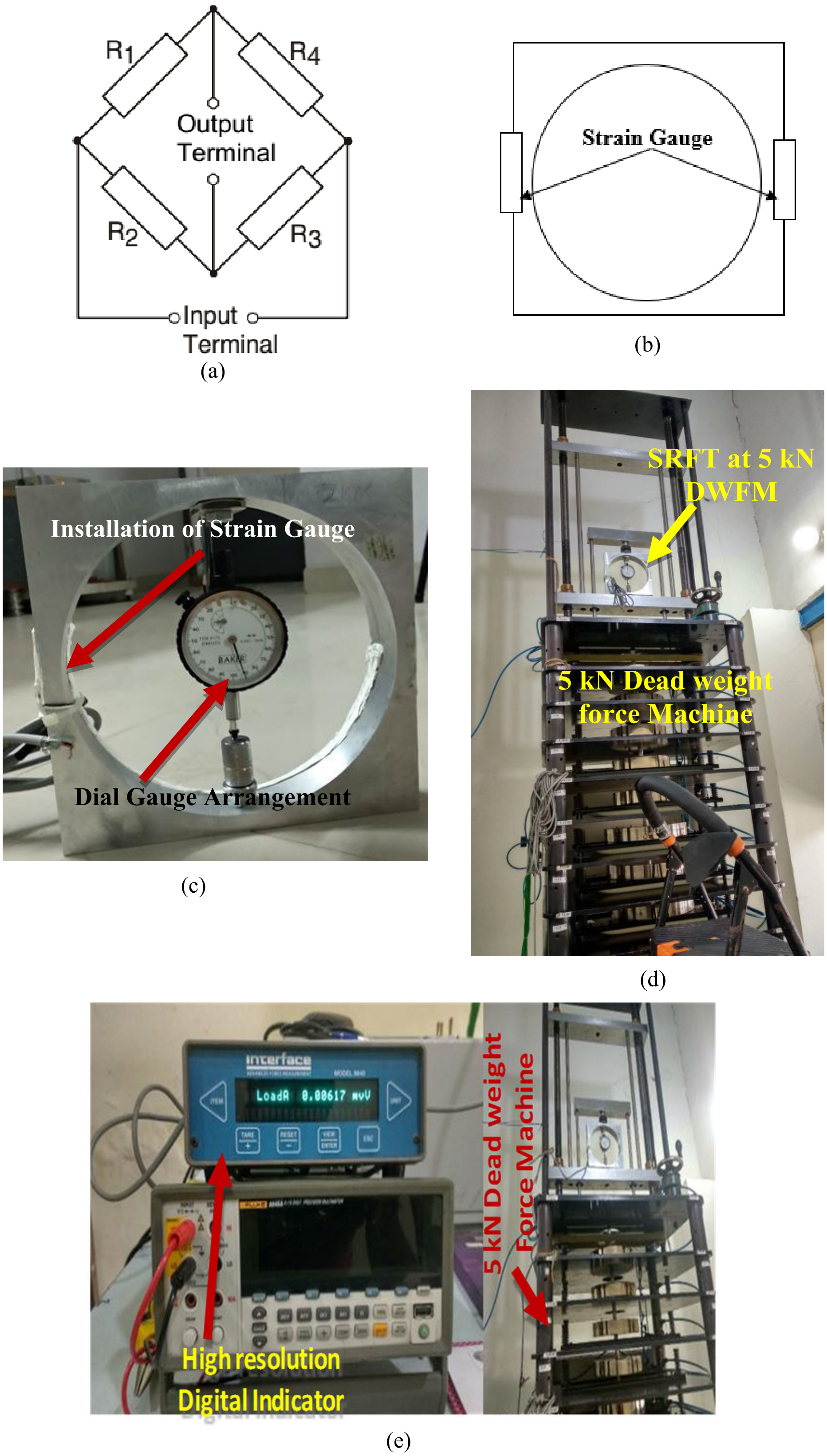

FIGURE 9. (a) Arrangement of strain gauge in wheatstone bridge form. (b) Location of strain gauge in SRFT. (c) Strain gauged SRFT. (d) 5 kN dead weight force machine. (e) Calibration with digital indicator of a SRFT.

TABLE 5. Deflection through different methods.

Sl. No.	Force (kN)	Deflection (mm) through different methods		
		Analytical	Computational	Experimental
1	0.2	0.054	0.065	0.059
2	0.4	0.108	0.130	0.120
3	0.6	0.162	0.195	0.178
4	0.8	0.216	0.260	0.238
5	1.0	0.270	0.325	0.298
6	1.2	0.324	0.390	0.358
7	1.4	0.378	0.455	0.419
8	1.6	0.432	0.520	0.480
9	1.8	0.486	0.585	0.540
10	2.0	0.541	0.649	0.599

TABLE 6. Difference in strain values using various methods.

Sr. No	Force (kN)	Analytical	Experiment	Mathematical model
1	0.2	0.11	0.10	0.10
2	0.4	0.23	0.20	0.20
3	0.6	0.34	0.30	0.29
4	0.8	0.46	0.40	0.40
5	1.0	0.57	0.51	0.51
6	1.2	0.69	0.61	0.60
7	1.4	0.8	0.71	0.71
8	1.6	0.92	0.81	0.81
9	1.8	1.03	0.91	0.90
10	2.0	1.15	1.02	1.01

force was evaluated by the mathematical model [33] as shown in Equation (15).

$$\frac{V_{out}}{V_{in}} = \frac{K\varepsilon\,(1+\mu)\,10^{-3}}{2} \tag{15}$$

Table 6 summarizes the voltage (mV/V) through the analytical computed strain and strain computed through computational method using Equation 15. The same is compared with the voltage output of the Wheatstone bridge when force is applied to the force transducer. The output of the Wheatstone bridge is measured through a precision digital indicator in mV/V. For rigorous and correct measurement of strain through FEA, the meshing and strain. Figure 14 summarizes the salient findings of Table 6.

III. METROLOGICAL INVESTIGATIONS

A calibration procedure has been adopted according to the ISO 376: 2011 standard for the calibration of the SRFT [34]–[36]. For the calibration of force transducer, a 5 kN dead weight force machine was used, having CMC $\pm$ 0.015 %. % ($k=2$) with room temperature at 23 °C $\pm$ 2 °C and a relative humidity of 50% $\pm$10%. The environmental conditions were maintained during the whole process of calibration.

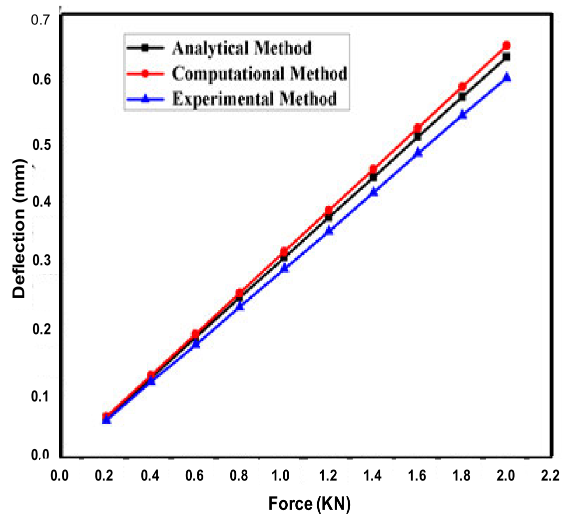

FIGURE 10. Comparison of deflection through different methods.

A. CALIBRATION PROCEDURE

As mentioned above, the force transducer has been calibrated following ISO 376: 2011 for its metrological characteristics and various factors have been evaluated for determination of the uncertainty measurement of the force transducer. A schematic representation of the calibration procedure is presented in Figure 15. The relevant factor has been discussed in detail previously [2]. Table 7 presents briefly the different factors contributing to the uncertainty of measurement of the force transducer, their method of computation, type of error (Type A/B), type of probability distribution, factor of division, etc. Relative uncertainty of measurement is evaluated as follows:

$$w_{ct} = \left(w_{re}^2 + w_{rp}^2 + w_{rs}^2 + w_{ze}^2 + w_{in}^2 + w_{re}^2 + w_{cr}^2\right)^{0.5} \tag{16}$$

Expanded uncertainty of measurement at $k = 2$, is evaluated as follows:

$$W_t = k.w_{ct} \tag{17}$$

Overall uncertainty of measurement is computed as follows:

$$W = (W_t^2 + W_{cmc}^2)^{0.5} \tag{18}$$

Factors contributing to the uncertainty of measurement of SRFT may be taken into account whether it is dial gauged SRFT or strain gauged SRFT.

B. METROLOGICAL CHARACTERIZATION OF STRAIN GAUGED SRFT

Table 8 summarizes the various factors contributing to the uncertainty of measurement of the SRFT, which is a vital indicator of metrological performance. Taking contributing

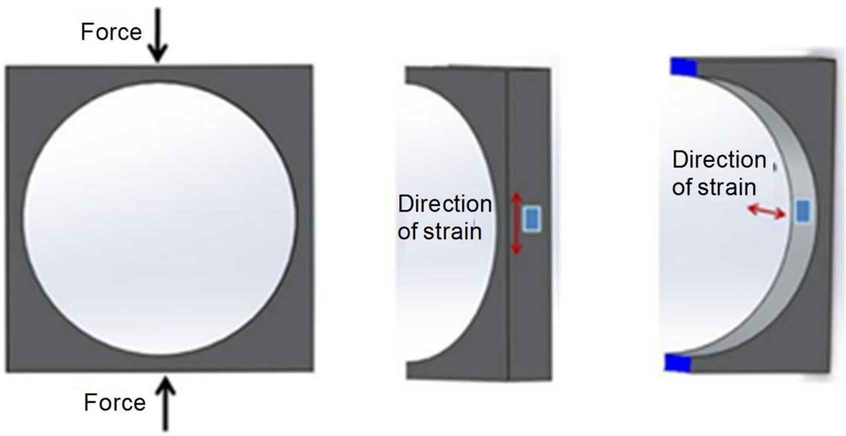

FIGURE 11. Force transducer with the strain gauge arrangement.

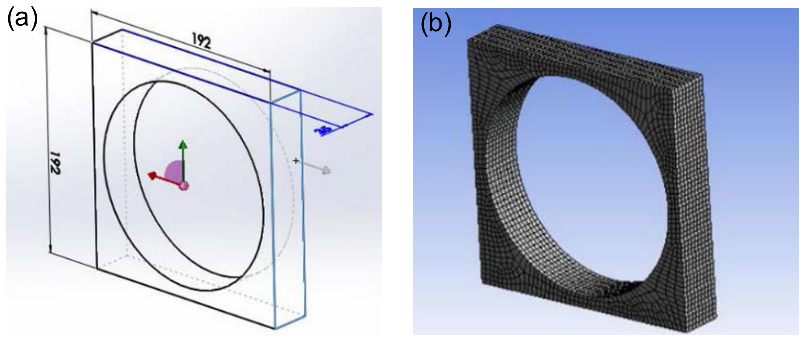

FIGURE 12. (a) Pictographic view of force transducer, (b) Meshing of the transducer.

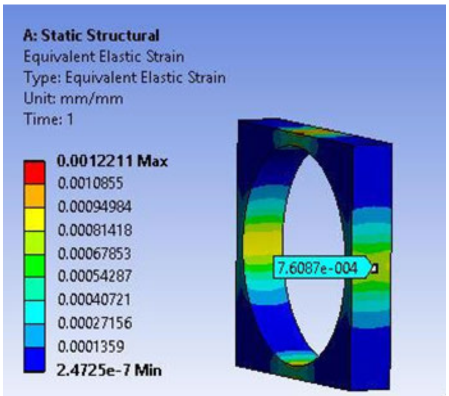

FIGURE 13. Maximum Strain value obtained under 2 kN Load.

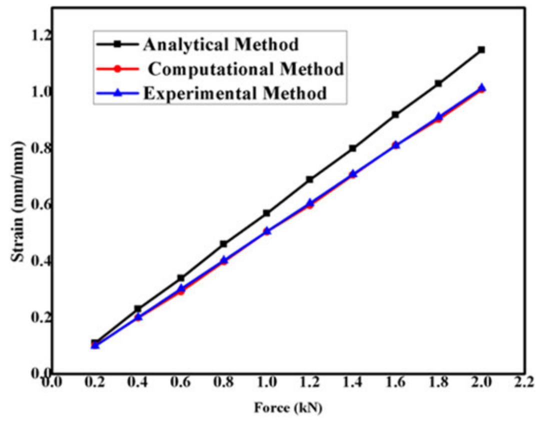

FIGURE 14. Comparison of strain through various methods.

factors from Table 7, it was found that the uncertainty of measurement is approximately 0.10 % ($k = 2$). This uncertainty is likely the result of relative uncertainties of reproducibility and reversibility are greater than or equal to 0.10 % (Figure 16). The force transducer falls under class D force transducers as per ISO 376: 2011.

C. PRACTICAL APPLICATION AND UTILIZATION OF THE DEVELOPED FORCE TRANSDUCER

The force transducer has varied utility for different industrial and metrological applications, including verification of uniaxial material testing and hardness machines and force transfer standards for static force measurement related applications. The strain gauged force transducer bears uncertainty of measurement well within limits established by standard calibration practices. The force transducer was used for verification of the uniaxial testing machine, as shown in Figure 17, up to a range of 5 kN. The force transducer bears uncertainty of measurement up to 0.05 % (in the range of 50 % - 100 % of nominal capacity) and can thus serve for precision force measurement applications. It is worth

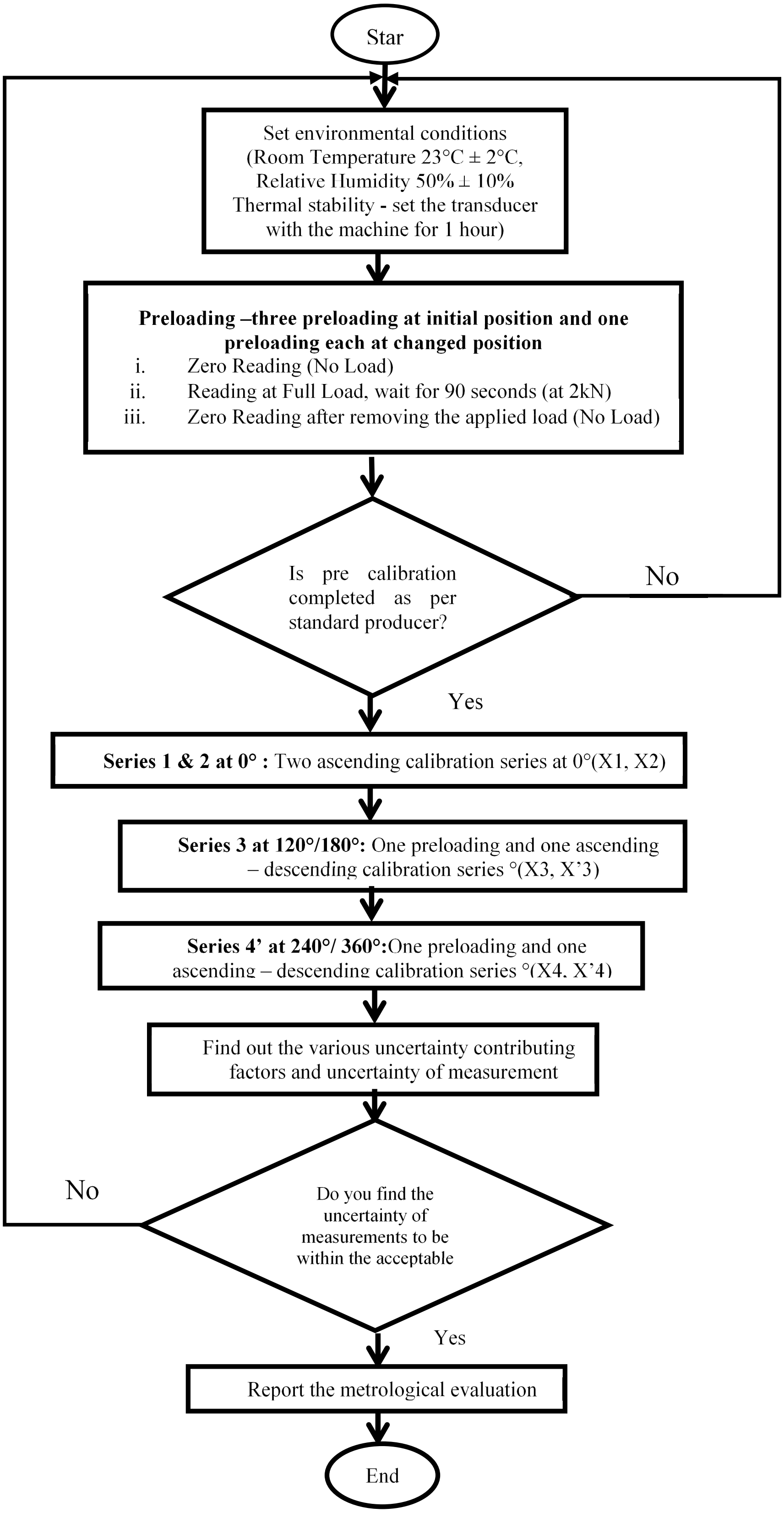

FIGURE 15. Calibration procedure flow diagram for a force transducer.

TABLE 7. Factors affecting uncertainty of measurement of a force transducer [33].

Sl. No.	Relative deviation due to (%) (2a)	Applicable for		Distribution type, Error and Factor of Division	Relative standard uncertainty contribution (w) % a/factor in previous column
		Force Proving Instrument (Dial gauged) (Yes/No)	Force Transducer (Strain gauged) (Yes/No)		
1	Zero offset	Y	Y	Rectangular, Type B, 1.732	a/1.732
2	Resolution	Y	Y	Rectangular, Type B, 2.449	a/2.249
3	Repeatability	Y	Y	Rectangular, Type B, 1.732	a/1.732
4	Reproducibility	Y	Y	U shaped, Type B, 2.449	a/2.449
5	Creep	Y	Optional	Rectangular, Type B, 1.732	a/1.732
6	Reversibility	N	Y	Rectangular, Type B, 1.732	a/1.732
7	Interpolation	N	Y	Triangular, Type B, 1.414	a/1.414
8	Applied force	Y	Y	Normal, Type B, 1	a

TABLE 8. Uncertainty of measurement of strain gauged force transducer with contributing factors.

Force (kN)	Relative uncertainty (10^{-2} %) due to							Uncertainty of measurement (10^{-2}, k = 2)
	Zero offset	Res.	Rep.	Rpr.	Int.	Rev.	Applied force	
0.2	1.3	1.0	4.0	6.9	1.2	9.9	1.5	7.5
0.4	1.3	0.5	3.5	6.4	0.2	6.7	1.5	6.0
0.6	1.3	0.3	3.3	5.3	1.1	6.8	1.5	5.8
0.8	1.3	0.2	2.7	5.2	0.1	6.6	1.5	5.6
1.0	1.3	0.2	2.4	4.4	0.0	5.2	1.5	4.9
1.2	1.3	0.2	1.8	3.8	0.3	5.0	1.5	4.6
1.4	1.3	0.1	1.6	3.4	0.3	4.2	1.5	4.3
1.6	1.3	0.1	1.2	2.6	0.1	3.2	1.5	3.8
1.8	1.3	0.1	1.0	2.4	0.2	2.0	1.5	3.5
2.0	1.3	0.1	0.9	1.6	0.0	0.0	1.5	3.2

mentioning that the force transducer has not been evaluated for dynamic force measurement related applications as there is no dynamic force measurement facility at the National Physical Laboratory, India (NPLI).

D. LIMITATIONS AND CHALLENGES

The developed force transducer offers several advantages but exhibits some limitations as well, which should be addressed and resolved in subsequent practical studies, whether for

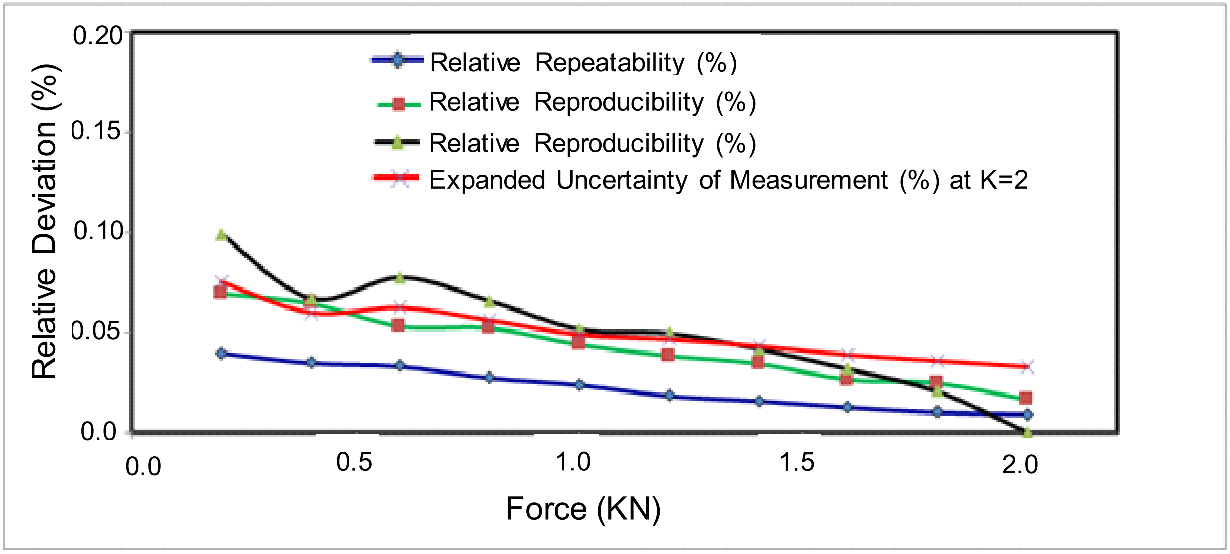

FIGURE 16. Uncertainty of measurement of strain gauged SRFT.

FIGURE 17. Verification of uniaxial testing machine.

commercial viability or applicability. The force transducer as discussed is of simple design and bears economical aspects while fabricating the same. This helps in breaking the trade barrier, while proposing an alternate to the commercial force transducers available. Though, there are some obvious advantages and features of a simple shaped force transducer as presented, but the force transducers bears following limitations and challenges:

1) DIMENSIONS

In its present form, the force transducer is comparatively large in comparison to commercially available alternatives. The current dimensions were chosen to be larger as the dial gauge required accommodation to validate deflection by experimental means, and no alternative economical solution was available. As coherence among the analytical, computational, and experimental approaches has been established, there is no need to verify the deflection in the future. Computational investigations (FEA) are sufficient to determine the capacity of the force transducer to be developed.

2) PRACTICAL VIABILITY

A force transducer was developed and its utility demonstrated for 2 kN in our current study. There is a need to develop the force transducer of a more conventional shape for a variety of capacities (e.g., 1–1 000 kN) for major metrological and industrial applications. Once developments in varying capacities are completed, the practical viability of the shape can be established.

3) ECONOMICAL CONSIDERATIONS

The force transducer developed is economical in comparison to comparable force transducers available commercially. Estimated cost of developed transducer approx. $200 – $300. There is need for further work to establish the economic viability of the presented force transducer.

4) DYNAMIC FORCE MEASUREMENT

With a growing need in this area, the force transducer developed is yet to be evaluated for dynamic force measurement. As there is no facility suited for dynamic force measurements at the National Physical Laboratory (NPL), India, evaluation of the force transducer for dynamic force measurement was beyond the scope of this work [35].

5) LONG-TERM STABILITY

Although the force transducer was evaluated repeatedly over several months and has stable metrological features, it has been observed that force transducer features have a tendency to deteriorate over a number of years. Hence, in order to prove the presented force transducer worthy, long-term stability study is required [36]–[37].

IV. CONCLUSION

The following conclusions may be drawn from the work presented here:

1) An SRFT was designed based on analytical and computational approaches followed by experimental measurements.

2)Al 7075 (T6) (aluminum alloy) was used as a material for the SRFT for a nominal capacity of 2 kN. The produced force transducer is strain gauged and falls under class D instruments as per ISO 376: 2011.

3) The SRFT has been investigated for its metrological characteristics as per ISO 376: 2011 using dial gauge (resolution 0.1 μm and 0.2 μm respectively) and strain gauges (resolution of digital indicator 0.00001 mV/V).

4) Metrological characterization reveals that the uncertainty of measurement of strain gauged SRFT is up to 0.05 % in the working range, making it suitable for industrial and metrological applications.

5) Attempts regarding optimization of dimensions and improvements in the uncertainty of measurement of SRFT are underway in order to present it as a commercially viable product.

ACKNOWLEDGMENT

The authors thank Dr. R. K. Agarwal, Director General and Prof. Ashiv Shah, Head, CORE, Ajay Kumar Garg Engineering College, Ghaziabad for all their support. They also Mr. Shanay Rab, Jamia Millia Islamia, New Delhi, for their valuable suggestions and support. They also would like to thank Editage (www.editage.com) for English language editing.

REFERENCES

[1] E. K. J. Chadwick and A. C. Nicol, "A novel force transducer for the measurement of grip force," *J. Biomech.*, vol. 34, no. 1, pp. 125–128, Jan. 2001.

[2] H. Kumar, C. Sharma, and A. Kumar, "The development and characterization of a square ring shaped force transducer," *Meas. Sci. Technol.*, vol. 24, no. 9, Jul. 2013, Art. no. 095007.

[3] J. Jin and C. Zhao, "Linear ultrasonic motor using quadrate plate transducer," *Frontiers Mech. Eng. China*, vol. 4, no. 1, pp. 88–91, Jan. 2009.

[4] R. Kumar, S. Rab, B. D. Pant, S. Maji, and R. S. Mishra, "FEA-based design studies for development of diaphragm force transducers," *MAPAN*, vol. 34, no. 2, pp. 179–187, Jun. 2019.

[5] D. Xu, Y. Wang, B. Xiong, and T. Li, "MEMS-based thermoelectric infrared sensors: A review," *Frontiers Mech. Eng.*, vol. 12, no. 4, pp. 557–566, Jun. 2017.

[6] R. Kumar and S. Maji, "Force transducers—A review of design and metrological issues," *Eng. Solid Mech.*, vol. 4, no. 2, pp. 81–90, Jan. 2016.

[7] T. Xu, H. Wang, Y. Xia, Z. Zhao, M. Huang, J. Wang, L. Zhao, Y. Zhao, and Z. Jiang, "Piezoresistive pressure sensor with high sensitivity for medical application using peninsula-island structure," *Frontiers Mech. Eng.*, vol. 12, no. 4, pp. 546–553, Dec. 2017.

[8] M.-H. Ho, P.-H. Lee, and P. Wang, "The research of low-profile load cell design sensitivity," *IOP Conf., Mater. Sci. Eng.*, vol. 423, Nov. 2018, Art. no. 012044.

[9] R. P. Ubeda, S. C. G. Rubert, R. Z. Stanisic, and Á. P. Ivars, "Design and manufacturing of an ultra-low-cost custom torque sensor for robotics," *Sensors*, vol. 18, no. 6, p. 1786, Jun. 2018.

[10] R. Arif, G. Fromentin, F. Rossi, and B. Marcon, "Mechanical analysis of local cutting forces and transient state when drilling of heat-resistant austenitic stainless steel," *Int. J. Adv. Manuf. Technol.*, vol. 104, nos. 5–8, pp. 2247–2258, Oct. 2019.

[11] R. Kumar, S. Rab, B. D. Pant, and S. Maji, "Design, development and characterization of MEMS silicon diaphragm force sensor," *Vacuum*, vol. 153, pp. 211–216, Jul. 2018.

[12] S. Rab, S. Yadav, R. K. Sharma, L. Kumar, V. K. Gupta, A. Zafer, and A. Haleem, "Development of hydraulic cross floating valve," *Rev. Sci. Instrum.*, vol. 90, no. 8, Aug. 2019, Art. no. 085102.

[13] X. Song, A. Li, M. Lv, H. Lv, and J. Zhao, "Finite element simulation study on pre-stress multi-step cutting of Ti-6Al-4V titanium alloy," *Int. J. Adv. Manuf. Technol.*, vol. 104, nos. 5–8, pp. 2761–2771, Oct. 2019.

[14] R. J. Godwin, "An extended octagonal ring transducer for use in tillage studies," *J. Agricult. Eng. Res.*, vol. 20, no. 4, pp. 347–352, Dec. 1975.

[15] J. Y. Sheikh-Ahmad, D. Ali, and F. Meng, "Design and implementation of a force dynamometer for friction stir welding," *Arabian J. Sci. Eng.*, vol. 43, no. 9, pp. 4649–4657, Sep. 2018.

[16] M. Liu, Q. Zhang, Y. Shao, C. Liu, and Y. Zhao, "Research of a novel 3D printed strain gauge type force sensor," *Micromachines*, vol. 10, no. 1, p. 20, Dec. 2018.

[17] B. Ravary, P. Pourcelot, C. Bortolussi, S. Konieczka, and N. Crevier-Denoix, "Strain and force transducers used in human and veterinary tendon and ligament biomechanical studies," *Clin. Biomech.*, vol. 19, no. 5, pp. 433–447, Jun. 2004.

[18] M. S. Uddin and D. Songyi, "On the design and analysis of an octagonal–ellipse ring based cutting force measuring transducer," *Measurement*, vol. 90, pp. 168–177, Aug. 2016.

[19] F. Becker, B. Lapatki, and O. Paul, "Miniaturized six-degree-of-freedom force/moment transducers for instrumented teeth with single sensor chip," *IEEE Sensors J.*, vol. 18, no. 6, pp. 2268–2277, Mar. 2018.

[20] *Button Load Cell (XBD): Miniature Load Cell*. Accessed: Feb. 22, 2020. [Online]. Available: https://www.800loadcel.com/load-cells/miniature-load-cells/miniature-button-load-cell.html

[21] *Compact Compression Load Cell, For Weigh Bridge*. Accessed: Feb. 22, 2020. [Online]. Available: https://www.indiamart.com/proddetail/compact-compression-load-cell-13468788548.html

[22] *Load Cell*. Accessed: Feb. 22, 2020. [Online]. Available: https://www.weighingsystem.in/load-cell.html

[23] A. Bray, "The role of stress analysis in the design of force-standard transducers," *Experim. Mech.*, vol. 21, no. 1, pp. 1–20, Jan. 1981.

[24] M. Prasad, N. Hasan, A. Kumar, and H. Kumar, "Design studies of a square ring shaped force sensor," *Int. J. Appl. Eng. Res.*, vol. 1, no. 4, p. 727, Oct. 2011.

[25] F. P. Beer, E. R. Johnston, and J. T. DeWolf, Eds., *Mechanics of Materials*, 4th ed. New York, NY, USA: McGraw-Hill, 2006.

[26] W. A. Nash, *Schaum's Outline of Theory and Problem of Strength of Materials*, 4th ed. New York, NY, USA: McGraw-Hill, Jul. 1998.

[27] M. A. Moazamand and M. Honarpsheh, "Ring-core integral method to measurement residual stress distribution of Al-7075 alloy processed by cyclic close die forging," *Mater. Res. Exp.*, vol. 6, no. 8, Jun. 2019, Art. no. 0865j3.

[28] N. M. Rahma, K. M. Eweed, and A. A. Mohammed, "Investigation and improvement the properties of 7075 AL/T6 alloy using TiO_2 nanomaterials," *IOP Conf., Mater. Sci. Eng.*, vol. 454, Dec. 2018, Art. no. 012144.

[29] L. Yagmur and B. Aydemir, "A comparative study for material selection of sensor element using analytic hierarchy process," *MAPAN*, vol. 33, no. 4, pp. 459–468, Dec. 2018.

[30] A. PratapSingh, S. K. Ghoshal, H. Kumar, and A. K. Rai, "Numerical investigation of square ring shape force transducer," *IOP Conf., Mater. Sci. Eng.*, vol. 561, Nov. 2019, Art. no. 012068.

[31] B. Chen, X. Wu, and X. Peng, "Finite element analysis of ring strain sensor," *Sens. Actuators A, Phys.*, vol. 139, nos. 1–2, pp. 66–69, Sep. 2007.

[32] K. Hoffmann, *Practical Hints for the Installation of Strain Gages*, 4th ed. Darmstadt, Germany: Hottinger Baldwin Messtechnik GmbH, HBM, 1996, pp. 1–56.

[33] *Surface Preparation for Strain Gage Bonding*, Measurements Group, Raleigh, NC, USA, 1976, Art. no. 27611.

[34] A. L. Window and G. S. Holister, Eds., *Strain Gauge Technology*. London, U.K.: Applied Science Publishers, 1982, pp. 1–356.

[35] Y. Fujii, "Toward establishing dynamic calibration method for force transducers," *IEEE Trans. Instrum. Meas.*, vol. 58, no. 7, pp. 2358–2364, Jul. 2009.

[36] *Metallic Materials-Calibration of Force-Proving Instruments Used for the Verification of Uniaxial Testing Machines*, Standard ISO 376:2011, Jun. 2011.

[37] H. Kumar, "A study of the long term stability of force transducers," *NCSLI Measure*, vol. 8, no. 4, pp. 40–44, May 2016.

AJAY PRATAP SINGH received the B.Tech. degree in mechanical engineering from Uttar Pradesh Technical University, Lucknow, India, in 2008, and the M.Tech. degree in fluids engineering from MNNIT, Allahabad, India, in 2010. He is currently pursuing the Ph.D. degree in mechanical engineering with IIT (ISM), Dhanbad, India. His research interests include design and development of force measurement devices, evaluation of material surface properties, simulation, fabrication of composite materials, and hydraulics and pneumatics.

SANJOY K. GHOSHAL received the Bachelor of Mechanical Engineering degree and the Master of Mechanical Engineering degree from Jadavpur University, Kolkata, India, in 1996 and 2003, respectively, and the Ph.D. degree in mechanical engineering from the Indian Institute of Technology, Kharagpur, India, in 2007. He is currently an Associate Professor with the Mechanical Engineering Department, Indian Institute of Technology (ISM), Dhanbad, India. His research interests include control theory, systems dynamics, modeling and simulation, robotics, fluid power and control, and measurement and metrology.

HARISH KUMAR received the B.Tech. degree in mechanical and automation engineering and the Ph.D. degree from GGS Indraprastha University, Delhi, India, in 2003 and 2015, respectively. From 2007 to 2017, he was a Scientist with the CSIR-National Physical Laboratory, New Delhi. He was a Guest Researcher with the National Institute of Standards and Technology, USA, in 2016. He is currently an Assistant Professor with the Department of Mechanical Engineering, National Institute of Technology Delhi. He has more than 35 publications to his credit, published in international peer-reviewed journals. His major research interests include mechanical measurement and metrology and composites. He has been serving as an editor of several peer-reviewed journals.

JONGHUN YOON received the Ph.D. degree from the School of Mechanical, Aerospace and System Engineering, KAIST, in 2008. He is currently a Professor with Hanyang University. His research interests include plasticity in metal forming, computational mechanics in metal forming, and mechanical properties at high-strain rate.

POONAM YADAV received the bachelor's degree in physics and mathematics and the master's degree from Deen Dayal Upadhaya University, Gorakhpur, India, in 2004 and 2006, respectively, and the Ph.D. degree in advanced materials science and engineering from Sungkyunkwan University, South Korea, in 2017. She is currently working as a Postdoctoral Fellow with the Mechanical Engineering Department, Hanyang University, ERICA, Ansan-si, South Korea. Her research interests include high temperature corrosion materials for industrial applications, fabrication of super hydrophobic surfaces by imprinting process, and coatings for corrosion protections.